Air-side performance of flat and corrugated fin-and-tube heat exchangers

A.H El Askary[a], M. K. Bassiouny[a], S. A. Wilson[a] and M.G. Demian[b]

[a] *Mechanical Power Eng. Dept., Faculty of Eng, Menofiya University, Shebin El-Kom, Egypt*
[b] *Technical institute, El-Mahalla, Egypt*

Experimental investigations of continuous flat and corrugated fin-and-tube heat exchangers are reported in this study. The heat exchangers consist of four fin-and-tube heat exchangers having plane fins and seven heat exchangers of corrugated fins with three staggered tube rows in the flow direction. The effect of fin spacing, the pattern depth and the corrugation frequency are investigated. For examining the influence of the number of tube rows on the Nusselt number, published experimental data are employed. Results are presented in terms of friction factor and Nusselt number. It is found that the friction factor decreases with the Reynolds number and increases with the fin spacing. The increase in both the pattern depth and frequency results in increasing the friction factor also. It can be concluded that the Nusselt number increases with Graetz number and pattern depth as well as the number of corrugation waves per tube row. From another hand, the Nusselt number decreases with increasing of both the fin spacing and the number of tube rows in the flow direction. General correlations for the friction factor and Nusselt number are proposed for the present fin configurations. These correlations, which are applicable to a wide range of varieties, are found to be representative of the experimental data with a good accuracy. Comparisons between the present correlations and those proposed by different authors are reported. A somewhat small discrepancy in the range of uncertainty of the previously published correlations is obtained. The proposed friction correlation can describe all the experimental results within ± 5 %, while the proposed heat transfer correlation can describe all the test data within ± 10 %.

تم فى هذه الدراسة تسجيل نتائج تجارب معملية أجريت على مبادلات حرارية ذات أنابيب وزعانف مستوية ومعرجة. تتكون المبادلات الحرارية المستخدمة فى الدراسة الحالية من أربعة نماذج ذات زعانف مستوية وسبعة نماذج ذات زعانف معرجة وتحتوى جميع النماذج على ثلاثة صفوف للأنابيب فى اتجاه السريان من النوع الموزع على شكل دلتا. وقد تم البحث عن تأثير المسافة البينية للزعانف وعمق التعاريج وعددها الخاص بكل صف من صفوف الأنابيب. كما تم استخدام بيانات معملية منشورة من أجل اختبار تأثير عدد صفوف الأنابيب على رقم نوسلت وقدمت النتائج فى صورة معاملات احتكاك ورقم نوسلت. وقد وجد أن معامل الاحتكاك يتناقص مع زيادة رقم رينولدز ويزداد مع تزايد المسافة البينية للزعانف. وقد أظهرت النتائج أن الزيادة فى كل من عمق التعاريج وعددها بكل صف يؤدى ايضا الى زيادة معامل الاحتكاك. وقد استنتج أن رقم نوسلت يزداد بزيادة رقم جراتس وعمق التعاريج وبالمثل فان زيادة عدد التموجات بين كل صفين من صفوف الأنابيب يؤدى الى نفس التأثير. ومن جهة اخرى يتناقص رقم نوسلت مع زيادة كل من المسافة البينية للزعانف وعدد صفوف الأنابيب فى اتجاه السريان. تم استنتاج معادلات تجريبية عامة لكل من معامل الاحتكاك ورقم نوسلت لأشكال الزعانف المستخدمة فى النماذج الحالية. وقد وجد أن هذه المعادلات التجريبية يمكن تطبيقها على مدى واسع من المتغيرات التى تعبر عن الأبعاد الأساسية للمبادلات الحرارية وكذلك ظروف تشغيلها وذلك بدقة عالية. وقد تم اجراء مقارنات بين المعادلات التجريبية الحالية والمعادلات المقترحة سابقا بواسطة باحثين اخرين. وقد وجد اختلاف بسيط نوعا ما يدخل فى نطاق اخطاء القياس المعملية للمعادلات التجريبية المنشورة سابقا. وقد تم التأكد أن المعادلة التجريبية لمعامل الاحتكاك يمكن أن تصف ١٠٠% من النتائج المعملية فى حدود ± ٥% بينما المعادلة التجريبية المستنتجة لانتقال الحرارة يمكن أن تصف جميع البيانات المعملية فى حدود ± ١٠%.

Keywords: Fin-and-tube heat exchanger, Corrugated fins, Flat fins, Air-side heat transfer coefficient

1. Introduction

Plate fin and tube heat exchangers have many applications, not only in the air-conditioning, heating and refrigeration industries, where their use is perhaps most common, but in several other industries as well. In air-conditioning, plate fin surface is

used extensively in packaged equipment for residential and commercial applications, room air–conditioners, induction and other terminal units, air-cooled condensers, transportation equipment and many others, too numerous to mention. In the electrical and mechanical equipment industries and the chemical process industry, plate fin surface is used for wide variety of heat transfer purposes. Examples are process gas heaters and coolers, compressors intercoolers and aftercoolers, oil coolers and solvent recovery heat exchangers.

In recent years, considerable interest has been focused on the techniques for augmenting convective heat transfer coefficients in heat transfer devices, as is evidenced by the surveys reported in [1,2]. In particular, augmentation techniques have been employed to improve the heat transfer performance of plate fin-and-tube heat exchangers. Such a heat exchnager consists of a set of equally spaced parallel plates of constant thickness and an array of tubes, which pass perpendicularly through the plates. Water, oils or refrigerants are forced to flow through the parallel tubes while air is directed across them. The most common augmentation technique for plate fin-and-tube heat exchangers is the use of corrugated fins instead of plane fins to effectively improve the air-side heat transfer coefficient. The corrugated fins are plates that have been fabricated with a periodic waviness in the streamwise direction. There are several variants of the basic wavy fin geometry. They may have a continuous wave configuration, or they may have herringbone wave configuration. External tube diameter from 9 to 15 mm, tube spacing from 19 to 40 mm, fin spacing from 1.6 to 4 mm, are the dimensions most frequently used. The number of rows is rarely more than 8 and air face velocity varies from 1 to 6 m/s.

Although a number of research works have been performed to investigate the heat transfer and pressure drop performances related to the geometry of the flat plate fin-and-tube heat exchangers particularly tube spacing, fin spacing and number of tube rows, only a limited number of publications are available on continuous corrugated fins.

Amano et al. [3] studied the turbulent heat transfer in corrugated-wall channels with and without fins. A numerical study is performed examining flow and heat transfer characteristics in a channel with periodically corrugated walls. The computations are made for several corrugation periods and for different Reynolds numbers. Xiao et al. [4] investigated the effect of interwall tube cylinder on the heat/mass transfer characteristics of corrugated plate fin-and-tube heat exchanger. They found that the interwall cylinder serves as a turbulence promoter. It enhances the heat/mass transfer in the low Reynolds number region. The existence of the interwall cylinder also causes the transition from laminar to turbulent to occur at lower Reynolds number. Goldstein and Sparrow [5] used the naphthalene sublimation technique to determine local air-side heat transfe coefficient for one row corrugated plate fin-and-tube heat exchangers. The same authors [6] also examined a corrugated duct, which did not contain the interwall cylinders, while the other configurations were the same as those in [5]. They found that the flow in the corrugated duct could be regarded as laminar up to Reynolds number 1200 (based on the hydraulic diameter). This implies that the existence of corrugation makes some contribution to the onset of turbulence.

Data on continuous ripped fins, which are performed to interrupted fins in applications where fouling by fibrous matter or insects is a problem, are available from Kays and London [7] and Maltson et al. [8]. Ghanem et al. [9] carried out an experimental study on fin coils with three different corrugation angles and fin spacings. They didn't investigate the effect of the fin frequency (i.e. the number of corrugations per tube row). Also, their suggested correlations hold only for corrugated fins and they didn't cover the case of flat fins. Rich [10] studied experimentally the effect of the number of tube rows on heat transfer performance of fin-and-tube heat exchangers but unfortunately he didn't construct any correlation for his measured data. Fifteen samples of plate fin heat exchangers with different geometrical parameters, including the number of tube rows, fin spacing and fin thickness are tested

and compared in an induced flow open wind tunnel by Wang et al. [11]. They found that the fin spacing does not affect the heat transfer coefficient. The number of tube rows has negligible effect on the friction factor and the fin thickness does not affect the heat transfer or friction characteristics. Rich [12] investigated a total of 14 coils, in which the fin spacing was varied from $W_f /D = 0.084$ to 0.64. He concluded that the heat transfer coefficient was essentially independent of the fin spacing. Chen and Ren [13] stated that the fin spacing does not affect the heat transfer coefficient for fin spacing ratio $W_f /D > 0.33$. On the contrary, the results of Elmahdy and Biggs [14] and Giovannoni and Mattarolo [15] showed that the j-factor increases as the number of fins per inch increases. They gave a unique correlation for the j-factor as a function of Reynolds number for each fin spacing considered. A heat transfer as well as a friction correlation for the wavy fin geometry is proposed by Wang et al. [16] indicating also the dependence of both the j-factor and the friction coefficient on the fin spacing. The experimental results of McQuiston and Tree [17] showed a decrease in the heat transfer coefficient with increasing the fin spacing. They also stated that the j-factor could be correlated by applying a correction "finning factor" defined as A / A_P to the Reynolds number. A strong dependence of the heat transfer coefficient and the finning factor was observed. McQuiston showed a $(A / A_P)^{-0.15}$ dependence in his plate-fin data. Kayansayan [18] indicated that the j-factor is proportional to $(A / A_P)^{-0.362}$. Two correlations for the air-side heat transfer coefficient and friction factor of flat plate fins were suggested by Gray and Webb [19]. Correlations were also developed by Webb [20] to predict the air-side heat transfer coefficient as a function of the flow conditions and geometric variables of heat exchangers having flat and wavy plate fins. These correlations were based on previously published experimental data by Beecher and Fagan [21].

In view of the wide-spread use of corrugated fin-and-tube heat exchangers, it is remarkable that there is a contrast between the results of the authors [11-17] especially for the case of fin spacing effect on the heat transfer coefficient. From another hand, despite there being some efforts devoted to the air-side performance [15, 20–24], significant differences of air-side performances took place perhaps owing to the raw data reduction method. Furthermore, very little or no information at all is available in the open literature about the dependence of the friction coefficient and Nusselt number on the wavy fin geometry such as the pattern depth and frequency. Therefore, the scope of the present paper is to carry out an experimental study on flat as well as corrugated fin-and-tube heat exchangers under varying fin spacing, pattern depth and corrugation frequency. In addition of this, to construct general correlations for estimating the friction coefficient, Nusselt number and Colburn factor in this type of heat exchangers as functions of the flow and geometry parameters based on a constant reduction method.

2. Experimental apparatus

The experimental test rig is designed to facilitate the measurements and control the thermo-fluid parameters through the heat exchanger models. Fig. 1 represents the layout of the test rig. The apparatus consists mainly of a rectangular air duct of 7.5x10.5 mm cross section and 1000 mm length. The air duct is used to direct the cooling air towards the test section which lies in the middle of the duct. The duct is manufactured from galvanized iron sheet with 0.8 mm thickness. Two layers of glass wool (25.4 mm thickness each) are used for insulating the outer duct surface. The fins are drilled in a way that lips are formed. The tubes are mounted inside the lips by interference, to insure a good thermal contact between the tubes and fins. The proposed fin and tube arrangement is shown in fig. 2. Eleven models with different geometrical configurations were used in the present study (as shown in table 1). All the models have three rows of tubes with staggered tube arrangement. Four of these models have flat fins and the others have corrugated fins. The corrugated fins geometry are shown in fig 2. The models have a transverse tube spacing S_n of 30 mm and the outer copper tube diameter D is 9.5 mm. The longitudinal tube spacing S_p

is 24 mm and the copper fin thickness is 0.15 mm. An electric heater of 30 Watt maximum power is fitted inside each copper tube. The heaters are connected to the electric power source in parallel. Because all the heaters have similar resistance, so they have the same power and emit the same amount of heat. A Variac transformer is used to control the power of heatres. The outer surface temperature of each tube is measured at the middle by using copper – constantan thermocouples of 0.2 mm wire diameter calibrated on a digital thermometer. The thermocouple is inserted in the inner side of the tube through a hole in its wall to measure the outer surface temperature. Because of the good contact between the tubes and fins, the wall temperature of tubes is considered as a base temperature for the fins. This base temperature is applied for calculating the film heat transfer coefficient h using the total surface efficiency η_t. The following

instruments were used for the control and the measurement purposes:

- An auto-transformer (variac transformer) is used for controlling the power supply to the electric heaters. The input voltage is 220 while the output varies from 1 to 220 volt.
- Digital thermometer, which capable on recording the temperature signals from the thermocouple probes in the range of –20 °C to 1370 °C with 0.1 °C resolution.
- Digital Wattmeter has measuring power range from 250 mW to 10 kW. Its accuracy is ± 0.15 W.
- An orifice meter for measuring the air flow rate. It has 7.5 mm inside diameter housed in a 12.5 mm diameter pipeline. The pressure difference across the orifice is measured by a mercury U-tube manometer.
- A U-tube manometer for measuring the pressure drop across the model. Water is used as the measuring fluid.
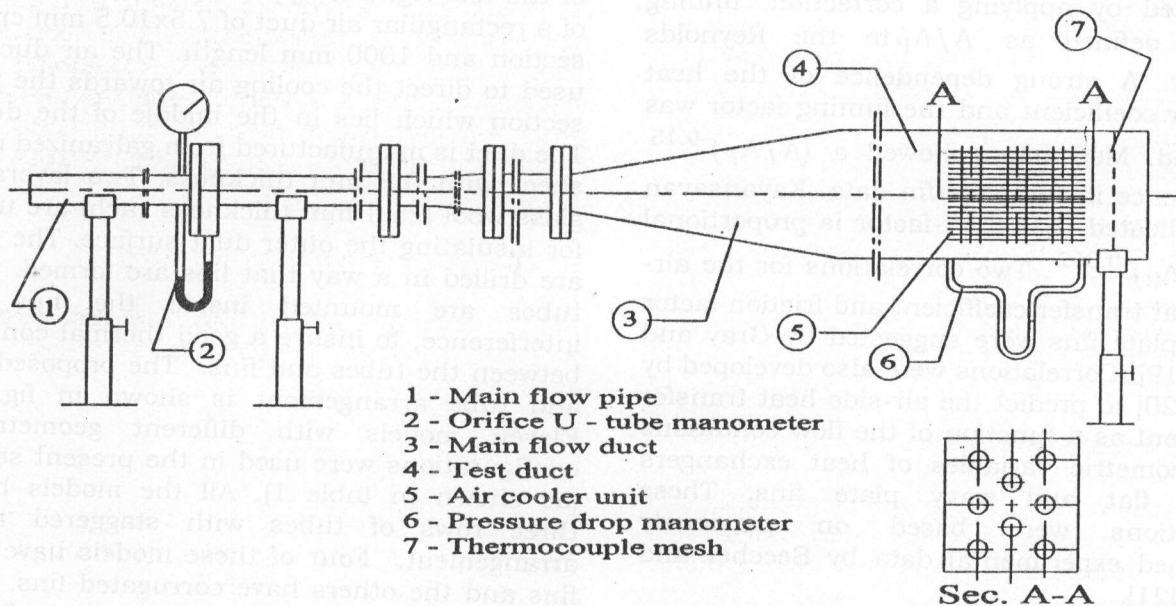- Bellows meter with 0.05 m³ resolution is used for calibrating the orifice meter.

1 - Main flow pipe
2 - Orifice U – tube manometer
3 - Main flow duct
4 - Test duct
5 - Air cooler unit
6 - Pressure drop manometer
7 - Thermocouple mesh

Sec. A-A

Fig. 1. Schematic diagram of the experimental set up.

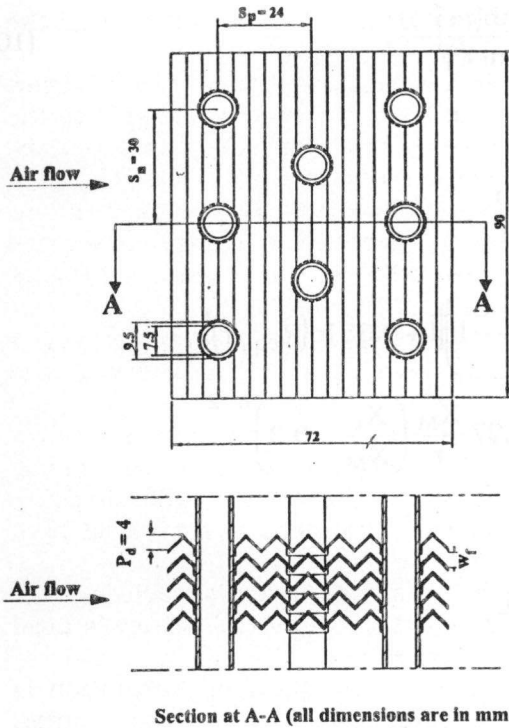Section at A-A (all dimensions are in mm.)

Fig. 2. Fin-and-tube arrangement as well as geometry of corrugated fins.

Table 1
Basic fin configurations

No	Feature	Fins density FPI (FPM)	Corrug. frequency per tube row	Corrug. depth (mm)
1	Flat	3 (118)	--	--
2	Flat	4 (157)	--	--
3	Flat	6 (236)	--	--
4	Flat	8 (315)	--	--
5	Corrugated	8 (315)	2	4
6	Corrugated	8 (315)	3	4
7	Corrugated	8 (315)	4	4
8	Corrugated	8 (315)	4	3
9	Corrugated	8 (315)	4	2
10	Corrugated	8 (315)	2	2
11	Corrugated	8 (315)	3	2

3. Experimental procedure

The cooling air flow rate is controlled via a throttle valve to the desired value. The orifice meter is calibrated by using the bellows meter and a stop watch for determining its coefficient of discharge C_d. Measuring the pressure drop across the orifice meter, the cooling air flow rate can be obtained as follows;

$$\dot{V} = C_d \, A_{or} \sqrt{2\frac{\Delta P}{\rho}} \, . \tag{1}$$

The electric heater is then put on and regulated to the desired power consumption by using the variac transformer. Air temperature measurements are carried out with the copper-constantan thermocouple probes. The entering air temperature is measured by a single thermocouple probe located about 250 mm upstream from the face of the heat exchanger. The hot air leaving the test section is measured with a multi-point grid located 500 mm downstream. Four points are used to obtain the average temperature for the exit hot air side. The average value is obtained as the arithmetic mean of the four thermocouple readings according to *ASHRAE* recommendation [25] as follows;

$$\overline{T}_o = \frac{1}{4} \sum_{j=1}^{j=4} (T_o)_j \, . \tag{2}$$

The thermocouple readings are observed periodically to check time dependent measurements. After reaching the steady state, all the measured variables are recorded.

Wall static pressure differential across the flow metering section is measured using a mercury U-tube manometer. The pressure drop across the test heat exchanger is measured using a water U-tube manometer, while inclined water manometer is used for measuring the small pressure drop across the test section.

4. Data reduction and processing

The average velocity of the air stream inside the duct is calculated using the equation

$$V_d = \dot{V}/A_d \, , \tag{3}$$

while the average air velocity flowing through the fins (maximum air velocity through the test section) is defined as follows:

$$V_f = V_d \, (A_d/A_{ff}) \, , \tag{4}$$

where A_{ff} is the minimum flow area in the test section. It depends on the fin thickness, fin density, tube diameter and the number of tubes per row. It can be calculated from the following equation;

$$A_{ff} = N_l \left(S_n - D \right) \left(H - n\, t \right). \tag{5}$$

The convective heat transfer coefficient across the test heat exchanger is calculated according to the following relation;

$$h = \frac{\dot{m}\, C_P\, \Delta T}{A\, \eta_t\, \theta}, \tag{6}$$

where η_t is the total surface efficiency [26]. It can be expressed mathematically as follows;

$$\eta_t = 1 - \frac{A_f}{A} \left(1 - \eta_f \right), \tag{7}$$

where,

$$A = A_f + A_P.$$

The value of A_f represents the surface area of fins. In case of corrugated fins, A_f can be defined mathematically according to the geometrical parameters represented in fig. 3 by the following equation;

$$A_f = 2n \begin{pmatrix} N_l S_n \times N_r S_p \times \sec(\alpha) - \frac{\pi}{4} D^2 N_t \times \sec(\alpha) \\ + t \left(N_l S_n + N_r S_p \times \sec(\alpha) \right) \end{pmatrix}. \tag{8}$$

The other term in the total heat transfer area A is the surface area of the tubes A_P uncovered by fins. This can be calculated from the following relation;

$$A_P = \left(H - n\, t \right) \left(\pi\, D\, N_t \right). \tag{9}$$

The fin efficiency, required for calculating the effective heat transfer area, is obtained by using the sector method, as described by Mcquiston and Parker [27] and Yu Chi et al. [28]. The efficiency is expressed as follows;

$$\eta_f = \frac{\tanh(m\, r\, \phi)}{m\, r\, \phi}, \tag{10}$$

where,

$$m = \sqrt{\frac{2\, h}{k\, t}},$$

$$\phi = \left(\frac{R_{eq}}{r} - 1 \right) \left[1 + 0.35 \ln\left(R_{eq} / r \right) \right];$$

$$\frac{R_{eq}}{r} = 1.27 \frac{X_M}{r} \left(\frac{X_L}{X_M} - 0.3 \right)^{1/2},$$

with,

$$X_M = \frac{S_n}{2},$$

and

$$X_L = \sqrt{\left(S_n / 2 \right)^2 + S_p^2} \; / 2.$$

3.1. Friction factor

Kays and London [7] gave a general definition for the friction factor in case of fin-and-tube heat exchangers. They proposed a formula containing the effect of the flow acceleration generated from the change in air density with temperature as follows;

$$f = \frac{A_{ff}}{A} \frac{v_i}{v_m} \left[\frac{2\, \Delta P}{G^2\, v_i} - \left(1 + \sigma^2 \right) \left(\frac{v_o}{v_i} - 1 \right) \right], \tag{11}$$

where,

$$\sigma = \frac{A_{ff}}{A_d}$$

is the ratio of the minimum flow area to the duct cross-sectional area at the test section,

$$G = \rho\, V_f$$

is the air mass velocity through the minimum flow area , and

$$v_m = \frac{v_i + v_o}{2},$$

where v_i and v_o are the specific volumes of air at inlet and outlet, respectively. In case of isothermal flow, eq. (11) is reduced to,

$$f = \frac{A_{ff}}{A}\left[\frac{2\,\Delta P}{V_f^2\,\rho}\right]. \tag{12}$$

The dimensionless groups used in the presentation of the present experimental data are defined in the following manner,

Reynolds number

$$Re = \frac{\rho\,V_f D_h}{\mu}. \tag{13}$$

Nusselt number

$$Nu = \frac{hD_h}{k}. \tag{14}$$

Stanton number

$$St = \frac{Nu}{Re\,Pr}. \tag{15}$$

Heat transfer factor (Colburn)

$$j = St\,Pr^{2/3}. \tag{16}$$

Graetz number

$$Gz = Re\,Pr\,\frac{D_h}{L_m}. \tag{17}$$

The hydraulic diameter as defined by Kays and London [7] is applied in the dimensionless numbers. Its value depends on the minimum flow area, the depth of heat exchanger in the flow direction and the total heat transfer area. It can be expressed as follows:

$$D_h = \frac{4A_{ff}L_m}{A}. \tag{18}$$

In terms of geometrical parameters for corrugated fins the hydraulic diameter becomes;

$$D_h = \frac{4N_r\left(S_n - D\right)\left(H - nt\right)\left(N_l S_p \sec(\alpha)\right)}{A}. \tag{19}$$

The fluid properties in the dimensionless groups are based on the arithmetic average of the entering and leaving air temperatures.

4. Results and discussion

In the present work, the performance of fin-and-tube heat exchangers is investigated to clear the relation between the friction loss as well as the heat transfer parameters and the heat exchanger geometries. In the following a brief description of the results is presented.

4.1. Friction factor

The experiments are carried out with extended air flow regime ranging from the laminar to turbulent flow based on the Reynolds number, as shown in fig. 3 for the effect of the fin spacing on the friction factor in case of flat fins. The staggered tubes arrangement leads to generate eddies and wakes behind the tubes. It is considered as a turbulence promoter even in low range of Reynolds number. In case of flat fins, the friction factor is found to be influenced by the fin spacing as appeared in fig. 4. The density of fins is varied as 3, 4, 6 and 8 FPI. It is clear that with increasing the fin spacing (i.e. decreasing the number of fins per inch), the air velocity past the fins decreases due to the corresponding increase in the flow area between the fins. This is reflected in turn on a significant reduction in the kinetic energy of cooling air and consequently on a considerable increase in the pressure. On another hand, the friction factor increases with decreasing the number of Fins Per Inch (FPI), as shown in fig. 3. This returns to the decrease of the flow velocity between the fins (i.e. increasing the flow area) with decreasing the number of fins per inch. The presence of the tube bank has a remarkable effect on the friction factor in connection with the fin density because the

friction factor across the tube bank depends mainly on the Reynolds number, which varies with the fin spacing.
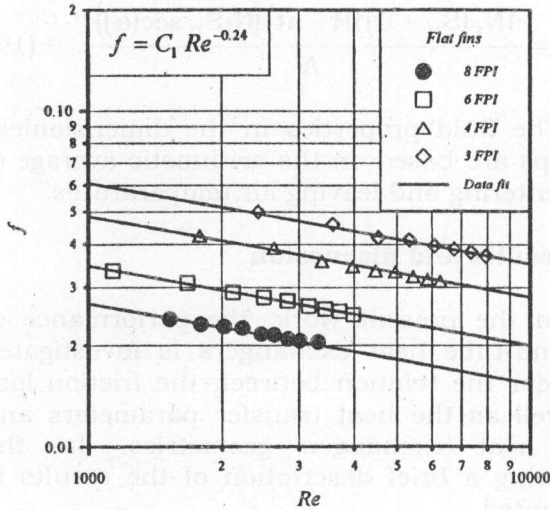

Fig. 3. Variatin of the friction factor with Reynolds number for different fin spacings in case of flat fins.
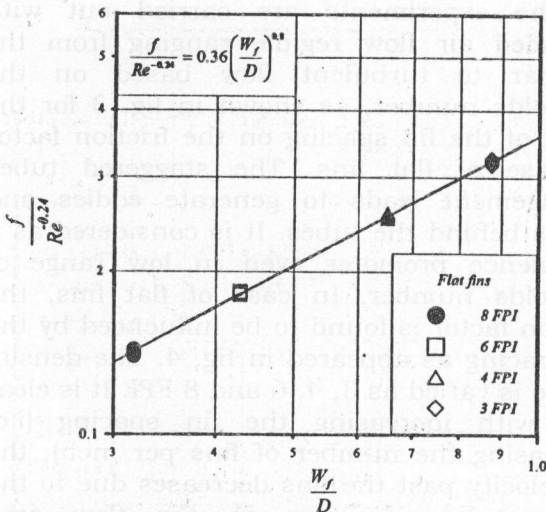

Fig. 4. Effect of fin spacing on the friction factor in case of flat fins.

It is seen that the friction factor has a constant slope on the log scale along the wide range of the Reynolds number. The power index of the Reynolds number that fits the measured data is obtained to be –0.24. The same result holds for corrugated fins as will be shown latter. Correlating the experimental data, the following formula is obtained for the friction factor of flat fins as a function of both the Reynolds number and the fin spacing.

$$f = 0.36 \, Re^{-0.24} \left(\frac{W_f}{D} \right)^{0.8} \tag{20}$$

Fig. 5 shows that the present correlation fits the experimental data fairly good . In case of corrugated fins, the effect of pattern depth is examined, as shown in fig. 6. The depth of corrugation is varied as zero (flat fins), 2, 3 and 4 mm, while the fins density is kept constant at 8 FPI. The experimental data are processed to correlate the effect of pattern depth on the friction factor as shown in fig. 7. It can be noticed from the figure that the friction factor increases with increasing the pattern depth which results in increasing the flow separation and consequently the eddies formation. As the fin spacing is kept constant, no significant change has been obtained in the kinetic energy of cooling air while the pressure drop increases with increasing the pattern depth. This behavior comes from the direct effect of two different factors. The first factor is due to the increase in the fin surface with increasing the pattern depth. The second one is due to the increase of the vortex size generated behind the corrugation steps as the pattern depth is increased. This in turn will increase the blockage effect to the main flow of the cooling air and consequently will increase the pressure loss.
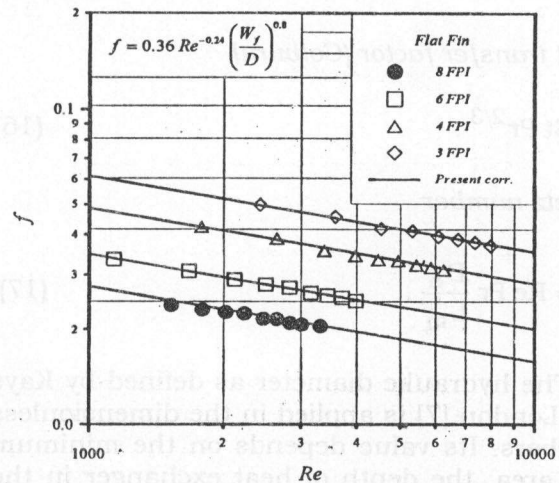

Fig. 5. Comparison between the test data and the present correlation for friction factor in case of flat fins.

The effect of corrugation frequency is also tested in the present work, as given by fig. 8. The fin spacing and pattern depth are kept

constant at 8 FPI and 4 mm respectively. The number of corrugation waves per tube row in the flow direction is varied as 0, 2, 3 and 4.
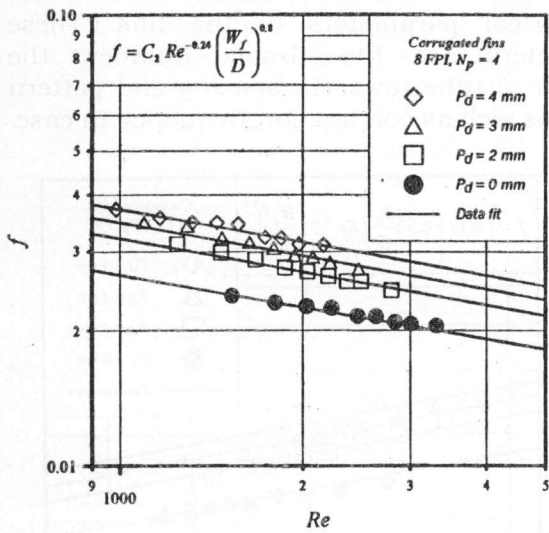

Fig. 6. Variation of the friction factor with Reynolds number for different pattern depths.
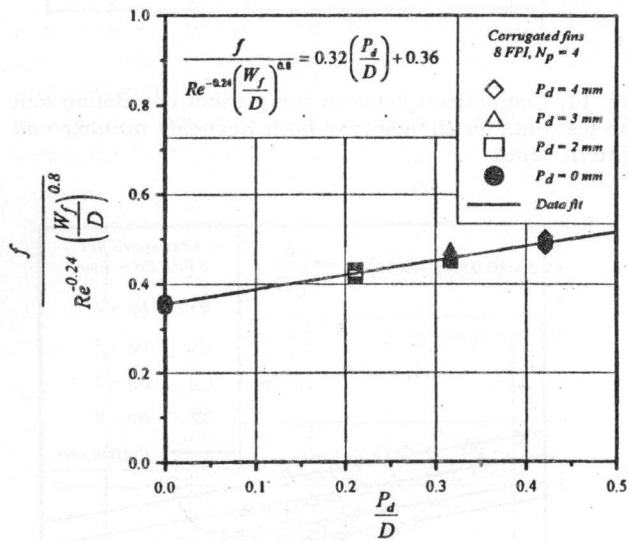

Fig. 7. Effect of pattern depth on the friction factor.

The zero corrugation frequency refers to flat fins. Because of the constancy of the pattern depth, it is believed that the turbulence intensity and eddies size are almost constant. The skin friction becomes the only factor, which has a significant contribution to the pressure drop. This interprets the slight increase in the friction

factor with respect to the number of corrugation waves belong to each tube row in the flow direction. This result appears clearly in fig. 9 in form of a low slope of the friction factor line against the corrugation frequency. This increase in the skin friction comes from the corresponding extension in the fins surface as a result of increasing the number of corrugation waves per tube row.
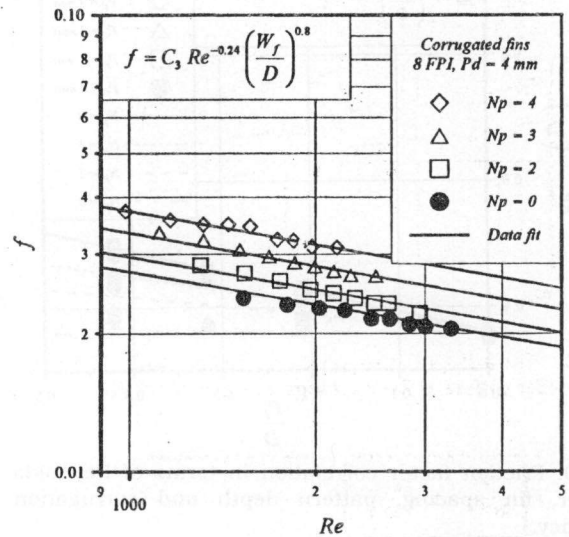

Fig. 8. Friction factor as a function of Reynolds number for different fin frequencies.
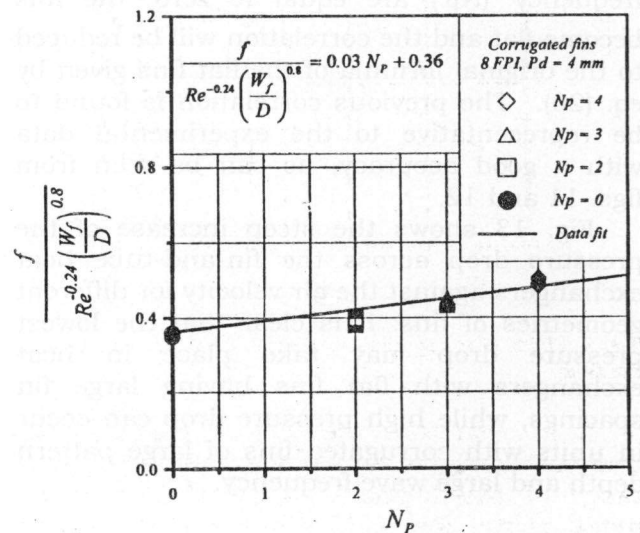

Fig. 9. Effect of the number of corrugation waves per tube row on the friction factor.

The correlation representing the effect of both the pattern depth and frequency is

derived from fig. 10 and it takes the following form;

$$f = \left[0.36 + 0.08\, N_P \left(\frac{P_d}{D} \right) \right] Re^{-0.24} \left(\frac{W_f}{D} \right)^{0.8}. \quad (21)$$
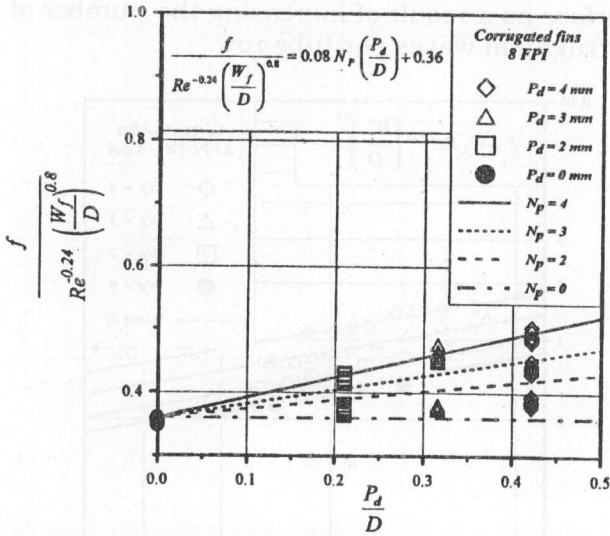

Fig. 10. Friction factor correlation in terms of Reynolds number, fin spacing, pattern depth and corrugation frequency.

When the pattern depth (P_d/D) and frequency (N_P) are equal to zero, the fins become flat and the correlation will be reduced to the original formula of the flat fins given by eq. (20). The previous correlation is found to be representative to the experimental data with a good accuracy, as can be seen from figs. 11 and 12.

Fig. 13 shows the steep increase of the pressure drop across the fin-and-tube heat exchangers against the air velocity for different geometries of fins. It is clear that the lowest pressure drop may take place in heat exchangers with flat fins having large fin spacings, while high pressure drop can occur in units with corrugated fins of large pattern depth and large wave frequency.

4.2. Heat transfer coefficient

Traditional heat exchanger calculations generally involve either the Log-Mean Temperature Difference (LMTD) method or the effectiveness $\in$-NTU method. Both methods require knowledge of the heat transfer

coefficient based on the logarithmic mean temperature difference. The present work aims to obtain general correlations on the air side heat transfer coefficient related to the flow and geometrical parameters of the fins. These parameters are the Graetz number, the number of tube rows, fin spacing and pattern depth as well as corrugation frequency in case
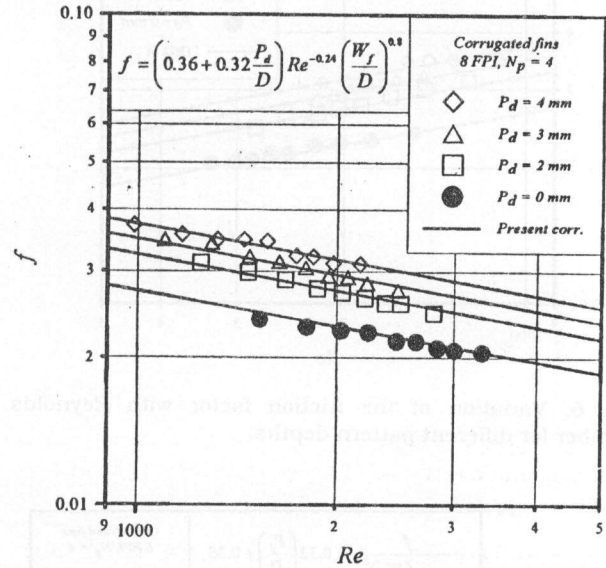

Fig. 11. Comparison between the present correlation and the test data for the effect of both Reynolds number and pattern depth
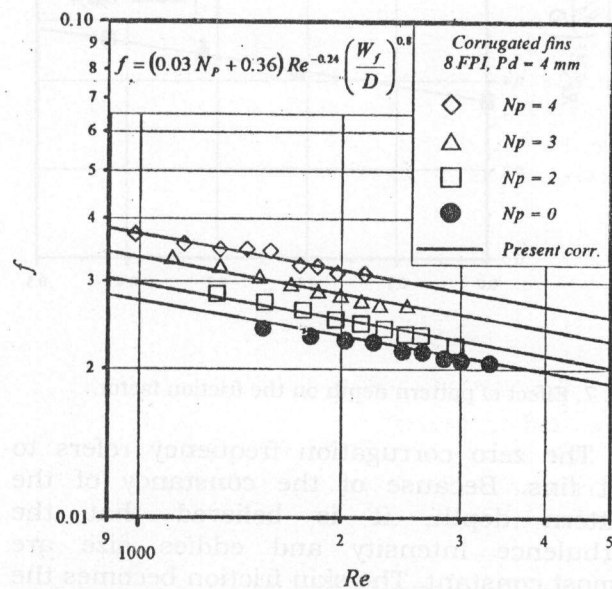

Fig. 12. Comparison between the present correlation and the experimental results for the influence of both Reynolds number and corrugation frequency.
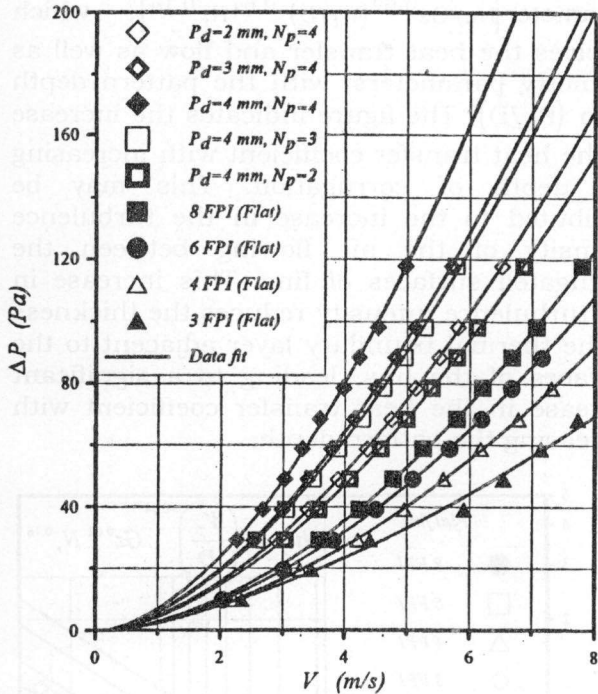
Fig. 13. Pressure drop across the fin-and-tube heat exchanger against the air velocity for different geometries of fins.

Fig. 14. Effect of the number of tube rows on the Colburn factor or Nusselt number.

of corrugated fins. The heat transfer factor (Colburn factor) and Nusselt number are used as dimensionless heat transfer coefficients.

For examining the effect of the number of tube rows on the Colburn factor or Nusselt number, the experimental results of Rich [10] are employed. In his experimental work he used flat fin models with different tube rows ranging from one row to six rows. Plotting his data in j-Re domain, as shown in fig. 14, the following relation is obtained.

$$j = \phi\left(N_r^{-0.16}\right). \qquad (22)$$

The foregoing correlation indicates the significant effect of the number of tube rows (N_r) on the heat transfer process in fin-and-tube heat exchangers.

The independent variable Graetz number Gz is chosen to represent the experimental data with the hydraulic diameter D_h as the characteristic dimension in the Reynolds number. The use of Graetz number as a correlating parameter makes it possible to combine the effect of Re, Pr and D_h/L_m into a single variable (the Graetz number).
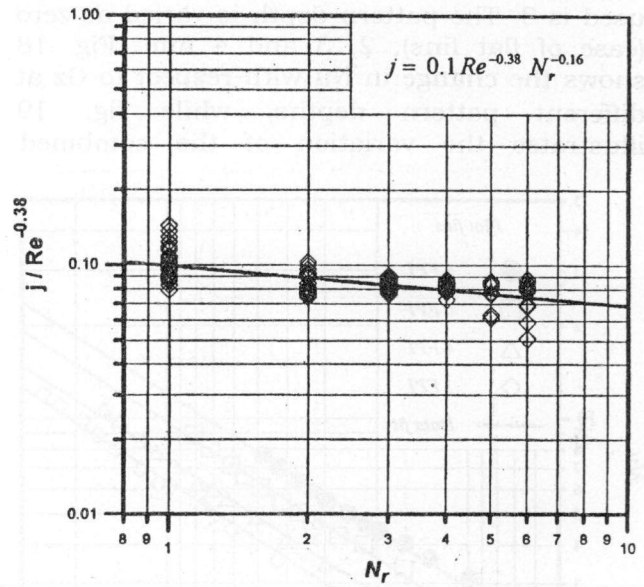
In case of flat fins, inspection of the plotted data in fig. 15 shows that the Nu vs. Gz logarithmic plot is linear. Hence, a constant exponent of 0.62 on Gz will accurately fit the data. It is also obvious from the experimental results represented by fig. 16 that a single straight line with a slope of –0.64 can be expected to describe satisfactorily the variation of Nusselt number with the fin spacing.

The resulting correlation for Nusselt number in case of flat fin geometry is listed below.

$$Nu = 0.39 \, Gz^{0.62} \left(\frac{W_f}{D}\right)^{-0.64} N_r^{-0.16}. \qquad (23)$$

Through the comparison of the previous developed correlation with the experimental data, a good agreement is obtained as may be seen from fig. 17.

The heat transfer process between the hot surfaces of fins and the cooling air is studied also in case of corrugated fin models. The effect of pattern depth on the heat transfer coefficient is investigated and evaluated under varying the air flow rate. During this study, the fin spacing and corrugation frequency as well as the number of tube rows are kept constant. This fin spacing is kept at 8 FPI,

while the corrugation frequency is fixed at 4 waves per tube row. The number of tube rows used is 3. The pattern depth is varied as zero (case of flat fins), 2, 3 and 4 mm. Fig. 18 shows the change in Nu with respect to Gz at different pattern depths, while fig. 19 illustrates the variation of the combined
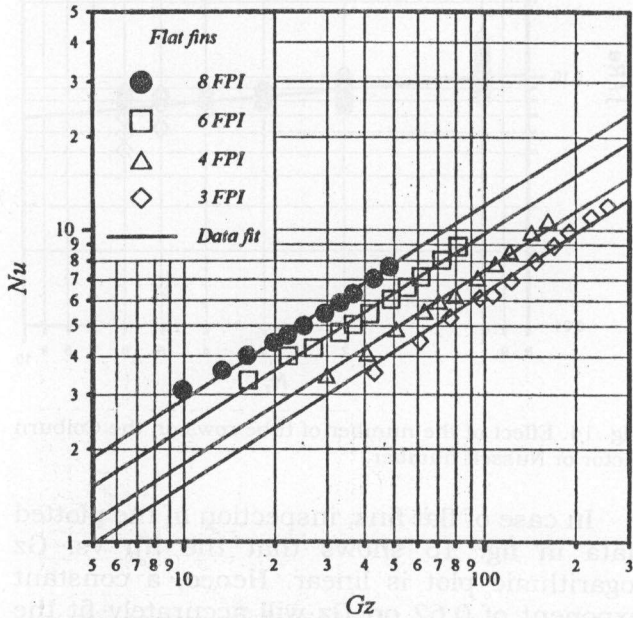
parameter $\left[Nu/Gz^{0.62}(W_f/D)^{-0.64}N_r^{-0.16}\right]$, which involves the heat transfer and flow as well as geometry parameters, with the pattern depth ratio (P_d/D). The figure indicates the increase in the heat transfer coefficient with increasing the depth of corrugation. This may be attributed to the increase in the turbulence intensity of the air flowing between the corrugated surfaces of fins. This increase in the turbulence intensity reduces the thickness of the thermal boundary layer adjacent to the surfaces of the fins, leading to a significant increase in the heat transfer coefficient with increasing the pattern depth.

Fig. 15. Variation of Nusselt number with the Reynolds number at different fin spacings in case of flat fins.
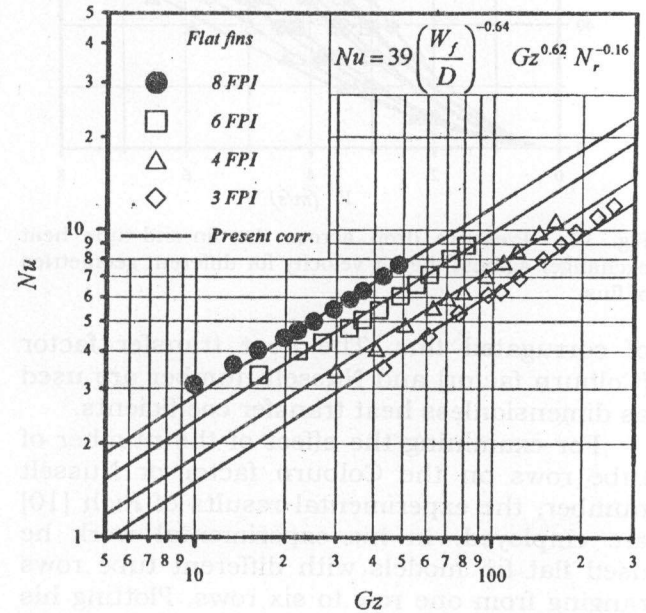
Fig. 17. Comparison of the present correlation for Nusselt number in case of flat fins with the test data.

The influence of corrugation frequency on the Nusselt number is also examined. For achieving this purpose, three corrugated fin-and-tube heat exchanger models are additionally manufactured with different corrugations per tube row. Thereby the pattern depth, the fin spacing and the number of tube rows in the flow direction are kept unchanged at 4 mm, 8 FPI and 3 tube rows, respectively. Fig. 20 represents the Nusselt number as a function of Graetz number under varying the corrugation frequency, while fig. 21 indicates the effect of the corrugation frequency on the thermal performance of fin-

Fig. 16. Effect of fin spacing on the Nusselt number in case of flat fins.

and-tube heat exchangers. The results show an increase in the Nu for corrugated fins over
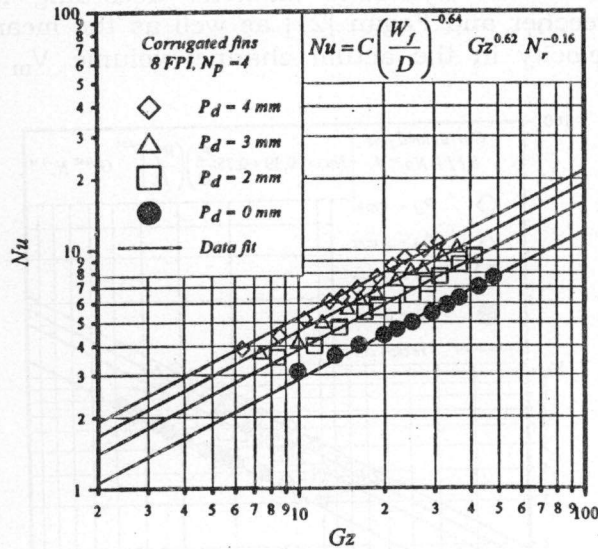
Fig. 18. Variation of Nusselt number with Graetz number for different pattern depths.
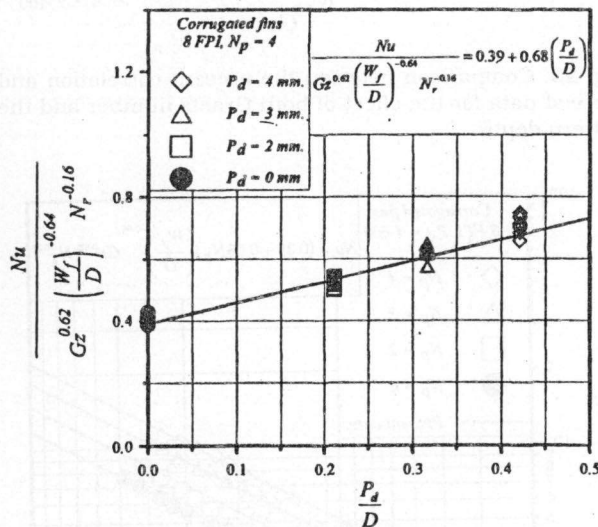
Fig. 19. Change of Nusselt number with the pattern depth ratio.

flat fins and this increase becomes more and more with increasing the number of corrugation waves per tube row. This may be due to the fact that corrugated fins accelerate the air flow, alternate the main flow direction, intensify the turbulence of the air flow between them and result in repeated (cyclic) flow. The wave length of corrugated fins depends on the number of corrugation cycles

and its amplitude depends on the pattern depth. Therefore, the corrugated fins enhance the heat transfer rate. The experimental data of the eleven fin and tube heat exchanger models, as given in table 1, are used for correlating the effect of both the pattern depth and corrugation frequency on Nusselt number, as shown in fig. 22. The resulting correlation is obtained to be as follows.

$$Nu = \left[0.39 + 0.17 \, N_P \left(\frac{P_d}{D} \right) \right] \times$$

$$Gz^{0.62} \left(\frac{W_f}{D} \right)^{-0.64} N_r^{-0.16} . \qquad (24)$$
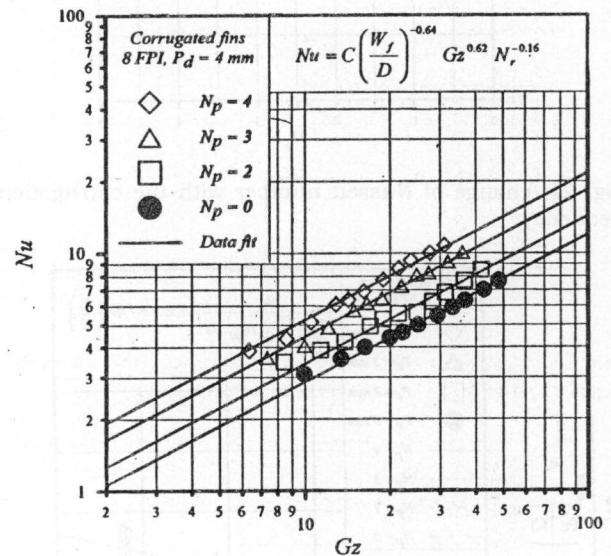
Fig. 20. Nusselt number as a function of Graetz number under varying the corrugation frequency.

The correlation is found to be fairly representative to the experimental data, as may be seen from figs. 23 and 24.

In form of Colburn factor, the foregoing correlation can be rewritten as follows;

$$j = \left[0.39 + 0.17 \, N_P \left(\frac{P_d}{D} \right) \right] \times$$

$$Re^{-0.38} \, Pr^{0.29} \left(\frac{D_h}{L_m} \right)^{0.62} \left(\frac{W_f}{D} \right)^{-0.64} N_r^{-0.16} . \qquad (25)$$

The variation of the air side heat transfer coefficient h with the air velocity V for the

different investigated fin patterns is indicated in fig. 25. The results show that high rates of heat transfer may be obtained using corrugated fins compared with flat fins especially for large pattern depth and frequency as well as small fin spacing.
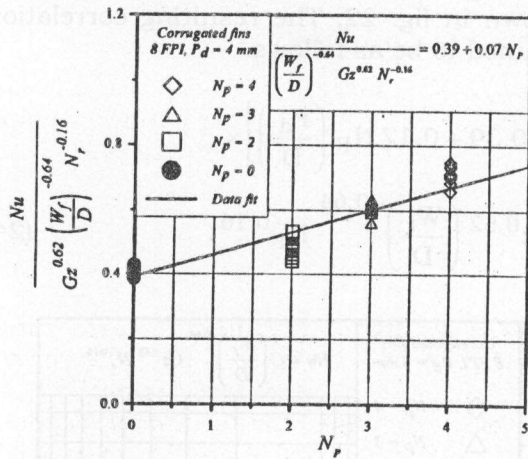
Fig. 21. change of Nusselt number with the corrugation frequency.
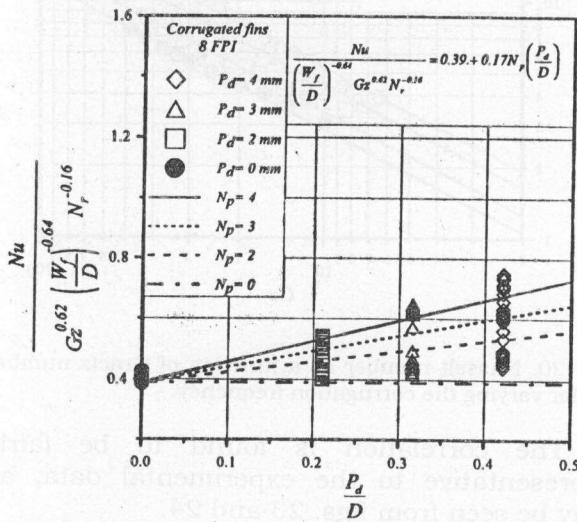
Fig. 22. Nusset number correlation in terms of Graetz number, fin spacing, number of tube rows, pattern depth and corrugation frequency.

4.3. Comparison between the present and previous work

The present general correlations, which are applicable to a wide range of varieties, are compared with correlations proposed by different authors for friction factor, Colburn

factor and Nusselt number. Because some authors used in their correlations the volumetric hydraulic diameter according to Beecher and Fagan [21] as well as the mean velocity in the actual channel volume V_m
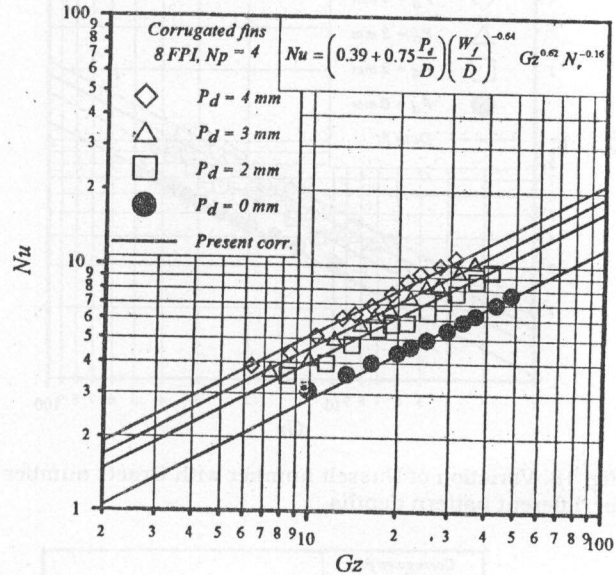
Fig. 23. Comparison between the present correlation and the test data for the effect of both Graetz number and the pattern depth.
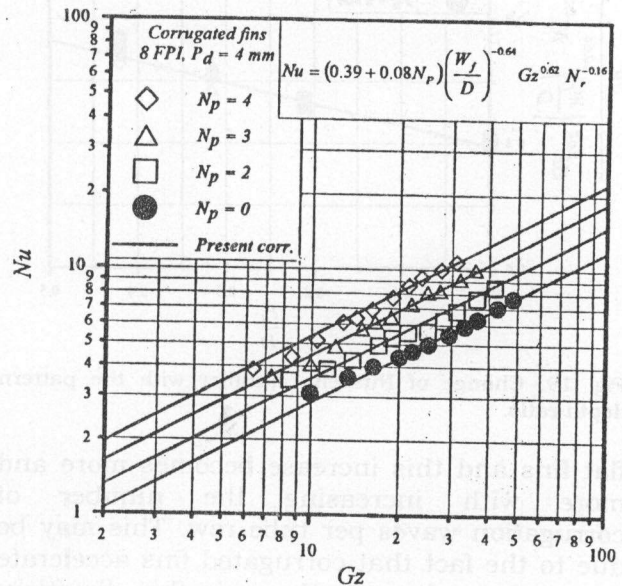
Fig. 24. Comparison between the present correlation and the experimental results for influence of both the Graetz number and the corrugation frequency.
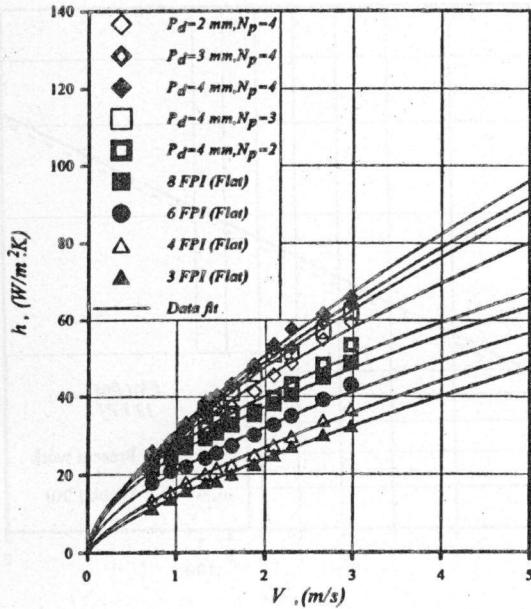
Fig. 25. Variation of the air-side heat transfer coefficient with the air velocity for different fin patterns.

instead of the maximum air velocity through fins V_f for defining Reynolds number Re^* and Graetz number Gz^*, the comparisons are based on these new definitions. The volumetric hydraulic diameter D_{hv} is defined mathematically as follows;

$$D_{hv} = 2 W_f (1-\beta) \Big/ \left[(1-\beta) \sec(\alpha) + 2\left(\frac{W_f \beta}{D_C}\right)\right]. \quad (26)$$

The Reynolds number Re^* is given by the following relation according to Beecher and Fagan [21],

$$Re^* = \frac{\rho V_m D_{hv}}{\mu}, \quad (27)$$

where

$$V_m = \frac{V_d \sigma_x}{(1-\beta)}, \quad (28)$$

$$\beta = \frac{\pi D_C^2}{4 S_n S_P}, \text{ and} \quad (29)$$

σ_x is the fin contraction ratio. It is defined as the fraction of the frontal area blocked by the fin thickness and it can be calculated from the relation;

$$\sigma_x = \frac{W_f}{W_f + t}. \quad (30)$$

Finally, the Graetz number Gz^* can be determined from the following equation using the definition of Beecher and Fagan [21].

$$Gz^* = Re^* Pr \frac{D_{hv}}{L_m}. \quad (31)$$

Fig. 26 compares the present correlation, represented by eq. (20), with those reported by Kays and London [7] and McQuiston [29] for the variation of the friction factor against Reynolds number in case of flat fins with 8 FPI fins density. As can be seen, the maximum deviation between the present correlation and the others is about 9%.

Another comparison between the present correlation, given by eq. (25), and the correlations of McQuiston [30], Kays and London [7] and Giovannoni [15] for the Colburn factor as a function of Reynolds number is shown in fig. 27. The comparison is done for flat fins of 8 FPI fins density. It is found that the experimental results of McQuiston as well as Kays and London are somewhat higher than those of the present work, while the results of Giovannoni are something lower than the present data.

A third comparison is made also between the present correlation for Nusselt number, eq. (23), and the correlation of Webb [20] in case of flat fins with 12 FPI fins density, as indicated in fig. 28. It is clear that the maximum deviation between both results is about 5%. This means that the valid range of the present correlation may be extended to cover density of fins up to 12 FPI.

The small discrepancy between the present data and the correlations of the above mentioned authors may be due to:
1. the data reduction method, for example the difference in fin efficiency calculation;
2. the uncertainty of the correlations of the different authors; for example in case of

McQuiston correlation [30] the uncertainty is reported to be ± 35 % at high density of fins; 3. the relative humidity of the flowing air between the fins as stated by ARI Standard [31] and Wang et al. [32].
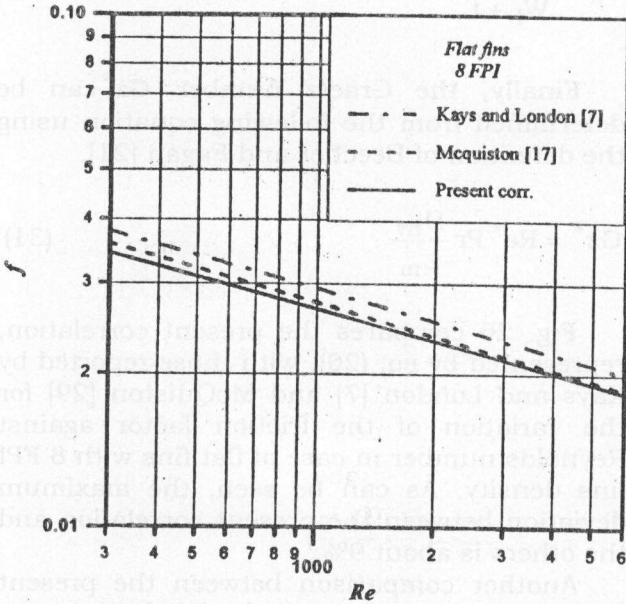
Fig. 26. Comparison between the present correlation for the friction factor and the correlations of another authors.
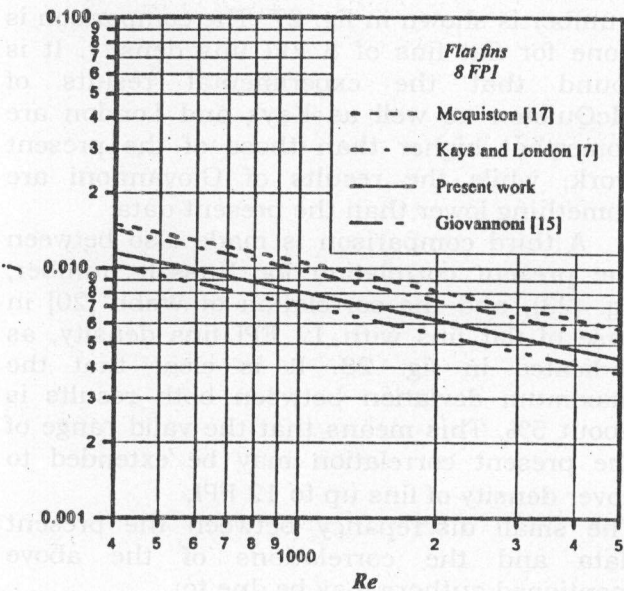
Fig. 27. Comparison between the present correlation for the Colburn factor and another previously published correlations.
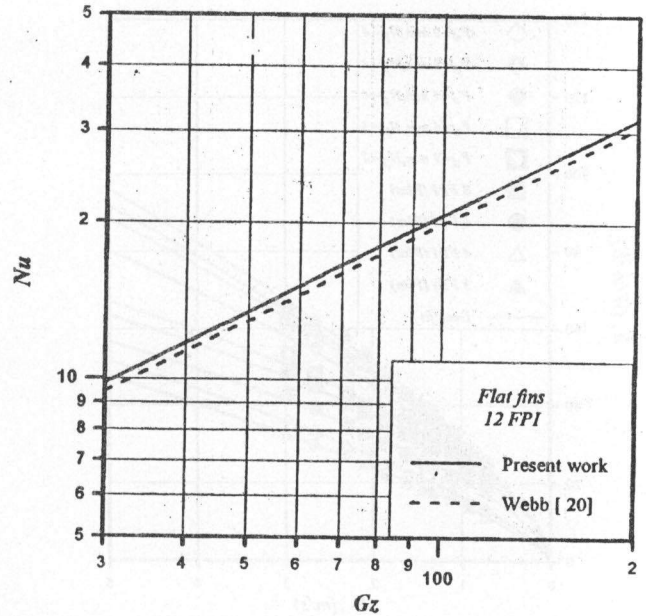
Fig. 28. Comparison between the present correlation for Nusselt number and that of Webb [20].

5. Conclusions

Experimental results are presented for eleven designs of fin-and-tube heat exchangers of different geometric configurations with both flat and corrugated fins. Correlations for friction factor, Nusselt number and Colburn factor are given as functions of the Reynolds number for friction factor or Graetz number in case of Colburn factor and Nusselt number as well as the geometric parameters of the heat exchangers. These correlations are believed to be more general and describe more test data from their earlier correlations.

On the basis of the previous discussion, the following conclusions are made:
1- The interwall tubes serve as turbulence promoters. They enhance significantly the heat transfer in the low Reynolds number region. The existence of the interwall tubes also causes the transition from laminar to turbulent to occur at lower Reynolds number.
2- The friction factor decreases with the Reynolds number, while it increases with fin spacing and pattern depth as well as corrugation frequency.
3- Nusselt number increases with Graetz number and pattern depth as well as with the number of corrugation waves. per tube row,

while it decreases with both fin spacing and the number of tube rows in the flow direction.

4- The proposed correlations for the present plate fin configurations can describe the friction factor test data within ± 5 % and the Nusselt number experimental results within ± 10 %.

5- The correlations show satisfactory agreement with the previously published correlations for flat fin-and-tube heat exchangers. Some earlier correlations give somewhat higher values, while another one yield close lower values.

Nomenclature

A	total heat transfer area, m^2
A_d	duct cross-section area at the test section , m^2
A_f	surface area of fins, m^2
A_{ff}	minimum free area for air through the fins, m^2
A_P	outer surface area of the tubes uncovered by fins, m^2
A_o	discharge area of the sharp edge orifice, m^2
C_d	coefficient of discharge for the orifice meter,
C_p	cific heat at constant pressure, J/kgK
D	tube outer diameter, m
D_C	collar diameter, m
D_h	hydraulic diameter, m
G	the air mass velocity through the minimum area, kg/m^2.s
Gz	Graetz number,
H	total height of the heat exchanger model, m
h	convective heat transfer coefficient, W/m^2 K
j	heat transfer factor (Colburn),
k	thermal conductivity, W/m.K
L_m	depth of heat exchanger in flow direction, m
N_1	number of tubes per row,
N_p	corrugation frequency (number of corrugation per tube row),
N_r	number of tube rows,
N_t	total number of tubes in the heat exchanger,
NTU	Number of Transfer Units,
Nu	Nusselt number,
n	total number of fins in the model, m
P_d	pattern depth, m
Pr	Prandtl number,
ΔP	pressure difference across the orifice meter, Pa
R_{eq}	equivalent radius for circular fin, m
Re	Reynolds number based on the hydraulic diameter,
r	tube inside radius, m
S_n	normal tube pitch, m
S_p	parallel tube pitch, m
St	Stanton number,
T	temperature, K
t	fin thickness, m
$\dot{V}$	air volume flow rate, m^3/s
V_d	average air velocity inside the duct, m/s
V_f	air velocity through fins, m/s
v	specific volume of air, m^3/kg
W_f	fin spacing, m
X_L	geometric parameter, m and
X_M	geometric parameter, m.

Greek letters

α	inclination angle of corrugation for fins, rad
Δ	difference,
θ	logarithmic mean temperature difference, K

$$\theta = \frac{\left[(T_{w,i} - T_{a,i}) - (T_{w,o} - T_{a,o})\right]}{\ln\left[(T_{w,i} - T_{a,i})/(T_{w,o} - T_{a,o})\right]}$$

η_f	fin efficiency,
η_t	total surface efficiency,
μ	dynamic viscosity of air, kg/m.s
ρ	air density, kg/m^3 and
σ	contraction ratio of the minimum flow

area to the duct cross-sectional area.

Subscript

a	air
d	duct
f	fin
h	hydraulic
i	inlet
l	longitudinal
m	mean
n	normal
o	outlet
or	orifice
P	tube
p	parallel
r	row
t	total
w	tube wall

Abbreviations

FPI	Fins per inch.
FPM	Fins per meter.

References

[1]   A.E. Bergles, "Survey and Evaluation of Techniques to Augment Convective Heat and Mass Transfer." Progress in Heat and Mass Transfer, Pergamon Press, Vol. 1, pp. 331-424 (1969).

[2]   A.E. Bergles, "Recent Developments in Convective Heat Transfer Augmentation." Applied Mechanics Reviews, Vol. 26, pp. 675-682 (1973).

[3]   R.S. Amano, A. Bagherlee, R.J. Smith and T.G. Niess, "Turbulent Heat Transfer in Corrugated-Wall Channels with and without Fins." Trans. ASME, Journal of H.T., Vol. 109, pp. 62-67 (1987).

[4]   Q. Xiao, B. Cheng and W.Q. Tao, "Experimental Study on Effect of Interwall Tube Cylinder on Heat/Mass Transfer Characteristics of Corrugated Plate Fin-and-Tube Heat Exchanger Configuration." Trans. ASME, Journal of H.T., Vol. 114, pp. 755-759 (1992).

[5]   L.J. Goldstein and E.M. Sparrow, "Experiments on the Transfer Characteristics of a Corrugated Fin and Tube Heat Exchanger Configuration."

Trans. ASME, Journal of H.T., Vol.98, pp.26-34 (1976).

[6]   L.J. Goldstein and E.M. Sparrow, "Heat/Mass Transfer Characteristics Flow in a Corrugated Wall Channel." Trans. ASME, Journal of H.T., Vol. 99, pp. 187-195 (1977).

[7]   W.M. Kays and A.L. London, "Compact Heat Exchangers." 3rd.ed., McGraw Hill, New York (1984).

[8]   J.D. Maltson, D. Wilcock and C.J. Davenport, "Comparative Performance of Rippled Fin Plate- Fin and Tube Heat Exchangers." Trans. ASME, Journal of H.T.,Vol. 111, pp. 21-28 (1989).

[9]   A.G. Ghanem, K.M. El-Shazly and A.S. El-Asfouri "Enhancement of Heat Transfer Through Fin-and-Tube Heat Exchangers Using Corrugated Fins." J. of Engng. And Applied Science, Cairo University, Faculty of Engng.,Vol 44 (2), pp. 309-324 (1997).

[10]   D.G. Rich, "The Effect of the Number of Tube Rows on Heat Transfer Performance of Smooth Plate Fin-and-Tube Heat Exchangers." ASHRAE Trans., Vol. 81, Part 1, pp. 307-317 (1975).

[11]   C. C. Wang, Y.J. Chang, Y.C. Hsieh and Y.T. Lin, "Sensible Heat and Friction Characteristics of Plate Fin-and-Tube Heat Exchangers Having Plane Fins." Int. J. Refrig., Vol. 19 (4), pp. 223-230 (1996).

[12]   D.G. Rich, "The Effect of Fin Spacing on the Heat Transfer and Friction Performance of Multi-Row, Smooth Plate Fin-and-Tube Heat Exchangers." ASHRAE Trans., Vol. 79, Part 2, pp.137-145 (1973).

[13]   Z.Q. Chen and J.X. Ren, "Effect of Fin Spacing on the Heat Transfer and Pressure Drop of a Two-Row Plate Fin and Tube Heat Exchanger." Int. J. Refrig., Vol. 11, pp. 456-460 (1988).

[14]   P.E. Elmahdy and P.E. Biggs, "Finned Tube Heat Exchangers: Correlation of Dry Surface Heat Transfer Data." ASHRAE Trans., Vol. 85, Part 2, pp. 262-273 (1979).

[15]   F. Giovannoni and L. Mattarolo, "Experimental Researches on the Finned Tube Heat Exchangers with Corrugated Fins." In Proceedings of the XVIth Int.

Congress of Refrigeration, Paris, Paper B. 1-493, pp. 215-220 (1988).

[16] C.-C. Wang, J.-Y. Jang and N.-F. Chiou, "A Heat and Mass Correlation for Wavy Fin-and-Tube Heat Exchangers" Int. J. Heat and Mass Transfer, Vol. 42, pp. 1919-1924 (1999)

[17] F.C. McQuiston and D.R. Tree, "Heat-Transfer and Flow-Friction Data for Two Fin-Tube Surfaces." Trans. ASME, Journal of H.T., Vol. 77, pp.249-250 (1971).

[18] N.Kayansayan, "Heat Transfer Characterization of Flat Plain Fins and Round Tube Heat Exchangers." Exper. Thermal Fluid Sci., Vol. 6, pp. 263-272 (1993).

[19] D.L. Gray and R.L. Webb, "Heat Transfer and Friction Correlations for Plate Finned-Tube Heat Exchangers Having Plain Fins." Proceedings of the 8th International Heat Transfer Conference, Vol. 6, pp. 2745-2750 (1986).

[20] R.L. Webb, "Air Side Heat Transfer Correlations for Flat and Tube Wavy Plate Fin-and-Tube Geometries." ASHRAE Trans., Vol. 96, Part 2, pp. 445-449 (1990).

[21] D.T. Beecher and T.J. Fagan, "Effects of Fin Pattern on the Air Side Heat Transfer Coefficient in Plate Finned-Tube Heat Exchangers." ASHRAE Trans., Vol. 93, Part 2, pp. 1961-1984 (1987).

[22] C.-C. Wang, W.L. Fu and C.T. Chang, "Heat Transfer and Friction Characteristics of Typical Wavy Fin-and-Tube Heat Exchangers." Experimental Thermal and Fluid Science,Vol. 14 (2), pp. 174-186 (1997).

[23] C.-C. Wang, Y.M. Tsi and D.C. Lu, "A Comprehensive Study of Convex-Louver and Wavy Fin-and-Tube Heat Exchangers." AIAA J. of Thermophysics and Heat Transfer Vol. 12 (3), pp. 423-430 (1998).

[24] M. Abu Madi, R.A. Johns and M.R. Heikal, " Performance Characteristics Correlation for Round Tube and Plate Finned Heat Exchangers." Int. J. Refrig., Vol.21 (7), pp. 507-517 (1998).

[25] ASHRAE Handbook of Fundamentals; American Society of Heating, Refrigerating and Air conditioning Engineers, New York (1993).

[26] F.P. Incropera and D.P. DeWitt, "Introduction to Heat Transfer" 2nd ed., John Wiley & Sons, Inc., Singapore (1990).

[27] F.C.McQuiston and J.D. Parker, "Heating, Ventilating and Air Conditioning" 4th ed., John Wiley & Sons, Inc., New York, Ch. 14, p. 571 (1994).

[28] Kuan-Yu Chi, Chi-Chuan Wang, Yu-Juei Chang and Yeon-Pun Chang, "A Comparison Study of Compact Plate Fin-and-Tube Heat Exchangers" ASHRAE Trans. Symposia, To-98-3-3, Vol. 104, Part 2, pp. 548-555 (1998).

[29] F. C. McQuiston, "Heat, Mass and Momentum Transfer Data for Five Plate-Fin Tube Transfer Surface". ASHRAE Transactions, Vol. 84, Part 1, pp.266-293 (1978)

[30] F. C. McQuiston, "Correlation of Heat, Mass and Momentum Transport Coefficient for Plate-Fin-Tube Heat Transfer Surface With Staggered Tubes" ASHRAE Transactions, Vol. 84, Part 2, pp. 294-309 (1978)

[31] ARI Standard, "Forced-Circulation Air-Cooling and Air-Heating Coils, Air-Conditioning". Refrigeration Institute, Arlington, VA, pp. 410-91 (1991)

[32] C.-C. Wang, Y.-C. Hsieh and Y.-T. Lin, "Performance of Plate Finned Tube Heat Exchangers Under Dehumidifying Conditions." Journal of Heat Transfer, Vol. 119, pp. 109-117 (1997).

Correlation for Round Tube and Plate Finned Heat Exchangers," Int. J. Refrig., Vol. 21 (7), pp. 507-517 (1998).

[25] ASHRAE Handbook of Fundamentals, American Society of Heating, Refrigerating and Air-conditioning Engineers, New York (1993).

[26] F.P. Incropera and D.P. DeWitt, "Introduction to Heat Transfer," 2nd ed., John Wiley & Sons, Inc., Singapore (1996).

[27] F.C. McQuiston and J.D. Parker, "Heating, Ventilating and Air Conditioning," 4th ed. John Wiley & Sons, Inc., New York, Ch. 14, p. 571 (1994).

[28] Kuan-Yu Chi, Chi-Chuan Wang, Yu-Juei Chang and Yeau-Ren Chang, "A Comparison Study of Compact Plate-Fin and-Tube Heat Exchangers," ASHRAE Trans. Symposia, To-98-5-3, Vol. 104, Part 2, pp. 548-555 (1998).

[29] F. C. McQuiston, "Heat, Mass and Momentum Transfer Data for Five Plate-Fin Tube Transfer Surfaces", ASHRAE Transactions, Vol. 84, Part 1, pp.266-293 (1978).

[30] F. C. McQuiston, "Correlation of Heat, Mass and Momentum Transport Coefficient for Plate-Fin-Tube Heat Transfer Surface With Staggered Tubes," ASHRAE Transactions, Vol. 84, Part 2, pp. 294-309 (1978).

[31] ARI Standard, "Forced-Circulation Air Cooling and Air Heating Coils," Air-Conditioning, Refrigeration Institute, Arlington, VA, pp. 410-91 (1991).

[32] C.C. Wang, Y.-C. Hsieh and Y.-T. Lin, "Performance of Plate Finned Tube Heat Exchangers Under Dehumidifying Conditions," Journal of Heat Transfer, Vol. 119, pp. 109-117 (1997).

Congress of Refrigeration, Paris, Paper B 1, 493, pp. 213-223 (1983).

[16] C.C. Wang, J.Y. Jang and N.F. Chiou, "A Heat and Mass Transfer for the Wavy Fin and Tube Heat Exchangers," Int. J. Heat and Mass Transfer, Vol. 42, pp. 1919-1924 (1999).

[17] F.C. McQuiston and D.R. Tree, "Heat Transfer and Flow Friction Data for Two Fin-Tube Surfaces," Trans. ASME, Journal of H.T., Vol. 77, pp.249-250 (1971).

[18] R.Karvinen, "Heat Transfer Characterization of Flat Plain Fins and Round Tube Heat Exchangers," Exper. Thermal Fluid Sci., Vol. 6, pp. 263-272 (1993).

[19] D.L. Gray and R.L. Webb, "Heat Transfer and Friction Correlations for Plate Finned-Tube Heat Exchangers Having Plain Fins," Proceedings of the 8th International Heat Transfer Conference, Vol. 6, pp. 2745-2750 (1986).

[20] R.L. Webb, "Air Side Heat Transfer Correlations for Flat and Tube Wavy Plate Fin-and-Tube Geometries," ASHRAE Trans., Vol. 96, Part 2, pp. 445-449 (1990).

[21] D.T. Beecher and T.J. Fagan, "Effects of Fin Pattern on the Air-Side Heat Transfer Coefficient in Plate Finned-Tube Heat Exchangers," ASHRAE Trans., Vol. 93, Part 2, pp. 1961-1984 (1987).

[22] C.-C. Wang, W.L. Fu and C.T. Chang, "Heat Transfer and Friction Characteristics of Typical Wavy Fin-and-Tube Heat Exchangers," Experimental Thermal and Fluid Science, Vol. 14 (2), pp. 174-186 (1997).

[23] C.-C. Wang, Y.M. Tsi and D.C. Lu, "A Comprehensive Study of Convex-Louver and Wavy Fin-and-Tube Heat Exchangers," AIAA J. of Thermophysics and Heat Transfer, Vol. 12 (3), pp. 423-430 (1998).

[24] M. Abu Madi, R.A. Johns and M.K. Heikal, "Performance Characteristics